

The Tris(trimethylsilyl)silylgallium Group as a Building Block in Gallium–Iron Clusters**

Gerald Linti* and Wolfgang Köstler

Abstract: Reaction of $[\{\text{Ga}(\text{Cl})\text{Si}(\text{SiMe}_3)_3\}_4]$ with the iron carbonylates $\text{Na}_2\text{Fe}(\text{CO})_4$, $\text{Na}_2\text{Fe}_2(\text{CO})_8$, and $\text{Na}_2\text{Fe}_3(\text{CO})_{11}$ affords derivatives of $\text{Fe}_2(\text{CO})_9$, in which either all, two, or one of the bridging CO ligands are replaced by the gallanediyl fragment $\text{GaSi}(\text{SiMe}_3)_3$. The Ga–Fe bond length in these compounds is 238 pm. This is shorter than the Ga–Fe single-bond length in bicyclic $[(\text{CO})_4\text{FeGa}_3(\text{OH})_4\{\text{Si}(\text{SiMe}_3)_3\}_3]$ ($d_{\text{Ga-Fe}} = 248.7$ pm) or in $[\{(\text{CO})_3\text{Fe}\}_2\{\text{GaSi}(\text{SiMe}_3)_3\}_2\text{Cl}]^-$ ($d_{\text{Ga-Fe}} = 245$ pm). The

latter is the chloride adduct of the $\text{Fe}_2(\text{CO})_9$ derivative with two bridging CO ligands substituted by $\text{GaSi}(\text{SiMe}_3)_3$. The description of these gallanediyl derivatives as CO analogues is supported by density functional calculations on gallane-substituted iron carbonyls. In the reactions mentioned above higher

Keywords: clusters • density functional calculations • gallium • iron • silicon

gallium–iron clusters with trigonal bipyramidal frameworks, which consist of two gallium and three iron atoms, are also formed. These are namely the anionic $[\{(\text{Me}_3\text{Si})_3\text{SiGa}\}_2\text{Fe}_3(\text{CO})_9\text{H}]^-$ and $[\{(\text{Me}_3\text{Si})_3\text{SiGa}\}_2\text{Fe}_3(\text{CO})_9\text{GaFe}(\text{CO})_4]^-$ clusters, which can be described according to Wade's rules as *closo*-clusters. The latter exhibits a gallium atom coordinated by three iron atoms: two $\text{Fe}(\text{CO})_3$ groups and a $\text{Fe}(\text{CO})_4$ fragment. The Ga– $\text{Fe}(\text{CO})_4$ bond may be compared with a metal–carbene bond.

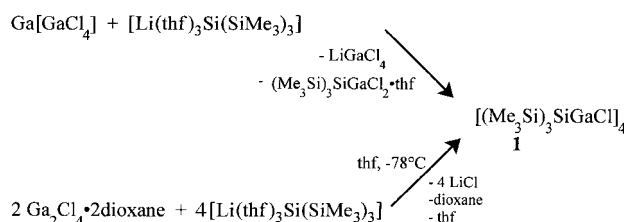
Introduction

Group 13 elements form a number of well-characterized compounds in which a $\text{M}(\text{CO})_n$ ligand is attached to the Group 13 atom.^[1] If we limit ourselves to the combination of gallium and iron, various compounds of the type $\text{X}_n\text{Ga}(\text{FeL}_x)_{3-n}$ are known. All of them are rationalized as trivalent gallium derivatives in which the metal–carbonyl ligand behaves as a pseudohalide. Examples are the series $[\{\text{CpFe}(\text{CO})_2\}_{3-n}\text{Ga}t\text{Bu}_n]$ ($n = 0, 1, 2$),^[2] $[(\text{CO})_4\text{Fe}\{\text{Ga}[(\text{CH}_2)_3\text{NMe}_2\text{R}]_2\}]_3$,^[3] anionic $[\{(\text{CO})_4\text{Fe}\}_2\text{GaMe}]^{2-}$,^[4] $[\{(\text{thf})\text{C}_2\text{H}_3\text{GaFe}(\text{CO})_4\}_2]$,^[5] and $[\{(\text{CO})_4\text{FeGa}[(\text{CH}_2)_3\text{NMe}_2]_2\}]_2$.^[6] The last two cases show the tendency of the gallium center to retain coordination number four; this is achieved by uptake of solvent molecules into the dimers of $[(\text{CO})_4\text{FeGaR}]$ ^[7] in which the GaR group serves as an isolobal analogue^[8] to a carbon monoxide ligand. For aluminum this analogy has recently been proven for $[(\text{CO})_4\text{FeAlCp}^*]$.^[9] Carbon monoxide can act as either a terminal or bridging ligand. The latter

bonding mode was observed for AlCp^* in $[(\text{CpNi})_2(\text{Cp}^*\text{Al})_2]$ ^[10] and for $\text{InC}(\text{SiMe}_3)_3$ in $[(\text{CO})_6\text{Fe}_2\{\text{InC}(\text{SiMe}_3)_3\}]$.^[11] In this report we describe the preparation and structures of gallium analogues to $[\text{Fe}_2(\text{CO})_9]$ and of higher gallium–iron cluster compounds starting from $[\{\text{Ga}(\text{Cl})\text{Si}(\text{SiMe}_3)_3\}_4]$ (**1**), in which the GaR group is viewed upon as a carbon monoxide analogue. This synthetic work is accompanied by quantum-chemical calculations which were carried out to verify the bonding situations in these compounds.

Results and Discussion

Synthesis of gallium–iron cluster compounds: Recently we have reported the synthesis of **1** by reaction of $\text{Ga}[\text{GaCl}_4]$ with $[\text{Li}(\text{thf})_3\text{Si}(\text{SiMe}_3)_3]$ (hypersilyl lithium)^[12] in medium yields (Scheme 1).^[13] Compound **1**, a bifunctional digallane with a



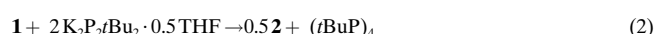
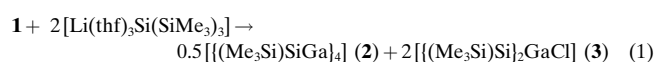
Scheme 1. Reaction scheme for the formation of **1**.

[*] Dr. G. W. Linti, Dipl.-Chem. W. Köstler
Institut für Anorganische Chemie der Universität Karlsruhe
Postfach 6980, Engesserstrasse, Geb. 30.45, D-76128 Karlsruhe
Fax: (+49) 721-608-4854
E-mail: linti@achpc9.chemie.uni-karlsruhe.de

[**] On the Chemistry of Gallium, Part 12. Part 11, see: G. Linti, W. Köstler, *Angew. Chem.* **1997**, *109*, 2758; *Angew. Chem. Int. Ed. Engl.* **1997**, *36*, 2644.

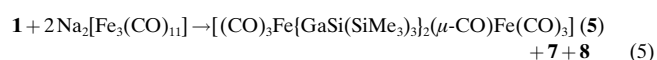
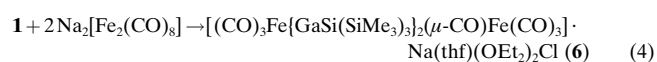
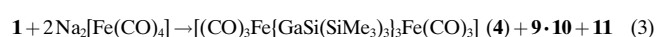
cuneane cage of four gallium and four chlorine atoms, is a promising molecule for synthesis of gallium cluster and ring compounds. Synthesis of **1** in nearly quantitative yields is achieved by addition of two equivalents of $[\text{Li}(\text{thf})_3\text{Si}(\text{SiMe}_3)_3]$ to a solution of $\text{Ga}_2\text{Cl}_4 \cdot 2$ dioxane in THF at -78°C .

Treatment of a solution of **1** in THF with $[\text{Li}(\text{thf})_3\text{Si}(\text{SiMe}_3)_3]$ in a molar ratio of 1:2 leads to dark violet crystals of the gallium(II) silyl **2** and yellow crystals of monomeric bis(hypersilyl)gallium chloride **3** [Eq. (1)].^[14] Evidently, chlorotris(hypersilyl)digallane is not stable towards disproportionation into gallium(II) and gallium(III) compounds; a property that has inherently been used in the preparation of **2** from $\text{Ga}_2\text{Cl}_4 \cdot 2$ dioxane and three equivalents of $[\text{Li}(\text{thf})_3\text{Si}(\text{SiMe}_3)_3]$.^[15] Compound **1** may even be reduced by $\text{K}_2\text{P}_2\text{tBu}_2$, whereby $(\text{PrBu})_4$ is formed along with **2** [Eq. (2)].



Both reactions indicate the promise of using **1** as a source for the gallium(II) fragment $\text{GaSi}(\text{SiMe}_3)_3$. Thus treatment of **1** with the reducing agent $\text{Na}_2\text{Fe}(\text{CO})_4$ affords the tris(hypersilyl)galliumdiiron hexacarbonyl cluster **4** [Eq. (3)], a diiron enneacarbonyl analogue in which the bridging CO ligands are replaced by $\text{GaSi}(\text{SiMe}_3)_3$. Compound **5**, which contains only two bridging $\text{GaSi}(\text{SiMe}_3)_3$ groups together with one bridging CO ligand, is expected to form when **1** is treated with the dinuclear carbonylate $\text{Na}_2\text{Fe}_2(\text{CO})_8$ [Eq. (4)]. In fact, **6**, which is a $\text{Na}(\text{thf})(\text{OEt})_2\text{Cl}$ adduct of **5**, is isolated. Treatment of **1** with $\text{Na}_2\text{Fe}_3(\text{CO})_{11}$ affords **5** along with a monogallyl derivative $[(\text{CO})_3\text{Fe}\{\text{GaSi}(\text{SiMe}_3)_3\}(\mu\text{-CO})_2\text{Fe}(\text{CO})_3]$ (**7**) [Eq. (5)].

Abstract in German: Die Reaktion von $[\{\text{Ga}(\text{Cl})\text{Si}(\text{SiMe}_3)_3\}_4]$ mit den Eisencarbonylarten $\text{Na}_2\text{Fe}(\text{CO})_4$, $\text{Na}_2\text{Fe}_2(\text{CO})_8$ und $\text{Na}_2\text{Fe}_3(\text{CO})_{11}$ liefert $\text{Fe}_2(\text{CO})_9$ -Derivate, in denen alle, zwei oder auch nur einer der verbrückenden CO-Liganden durch das Gallandiyl-Fragment $(\text{Me}_3\text{Si})_3\text{SiGa}$ ersetzt sind. Die GaFe-Abstände in diesen Verbindungen betragen 238 pm. Sie sind deutlich kürzer als die GaFe-Einfachbindungen im bicyclischen $[(\text{CO})_4\text{FeGa}_3(\text{OH})_4\{\text{Si}(\text{SiMe}_3)_3\}_3]$ ($d_{\text{Ga-Fe}} = 248.7$ pm) oder in $[\{(\text{CO})_3\text{Fe}\}_2\{\text{GaSi}(\text{SiMe}_3)_3\}_2\text{Cl}]^-$ ($d_{\text{Ga-Fe}} = 245$ pm). Letzteres ist das Chloridaddukt des $\text{Fe}_2(\text{CO})_9$ -Derivates, in dem zwei der verbrückenden CO-Liganden ersetzt sind. Die Beschreibung dieser Gallandiyl-Komplexe mit Eisencarbonylfragmenten als CO-Analoga wird durch parallel durchgeführte Dichtefunktionalrechnungen unterstützt. In den oben erwähnten Reaktionen werden auch höhere Gallium-Eisen-Cluster mit trigonal-bipyramidalen Gerüsten aus zwei Gallium- und drei Eisen-Atomen gebildet. Dies sind die Clusteranionen $[\{(\text{Me}_3\text{Si})_3\text{SiGa}\}_2\text{Fe}_3(\text{CO})_9\text{H}]^-$ und $[\{(\text{Me}_3\text{Si})_3\text{SiGa}\}_2\text{Fe}_3(\text{CO})_9\text{GaFe}(\text{CO})_4]^-$, die gemäß den Wade-Regeln als closo-Cluster beschrieben werden können. Das zweite Clusteranion enthält ein durch zwei $\text{Fe}(\text{CO})_3$ -Gruppen und ein $\text{Fe}(\text{CO})_4$ -Fragment dreifach koordiniertes Galliumatom. Die $\text{GaFe}(\text{CO})_4$ -Bindung kann mit den Bindungen in Metall-Carben-Komplexen verglichen werden.



However, the main product of this reaction is the anionic digallium–triiron cluster $[\{(\text{CO})_3\text{Fe}\}_3\{\text{GaSi}(\text{SiMe}_3)_3\}_2\text{H}]^- [\text{Na}(\text{triglyme})]^+$ (**8**). The anionic gallium–iron cluster $[\{(\text{CO})_3\text{Fe}\}_3\{\text{GaSi}(\text{SiMe}_3)_3\}_2\{\text{GaFe}(\text{CO})_4\}]^-$ (**9**), which is similar to **8**, is a minor by-product in the reaction given in Equation (3) if hydroxide-containing $\text{Na}_2\text{Fe}(\text{CO})_4 \cdot 2$ dioxane is used. The counterion is $[\{(\text{Me}_3\text{Si})_3\text{Si}\}_4\text{Ga}_4\text{O}(\text{OH})_5]^+$ (**10**) with an adamantoid gallium oxo/hydroxy cage. A further by-product in this reaction is $[\{(\text{Me}_3\text{Si})_3\text{Si}\}_3\text{Ga}_3(\text{OH})_4\text{Fe}(\text{CO})_4]$ (**11**). Here two hydroxyl groups of trimeric $[\{(\text{Me}_3\text{Si})_3\text{Si-Ga}(\text{OH})_2\}_3]$ are substituted by an $\text{Fe}(\text{CO})_4$ group.

Spectroscopic characterization of 4–7: The IR spectrum of **4** exhibits only two absorptions for terminal CO ligands in the carbonyl region ($\tilde{\nu} = 1964$ and 1921 cm^{-1}) in accordance with a D_{3h} symmetric molecule. The red shift of 100 cm^{-1} compared with the signal for $\text{Fe}_2(\text{CO})_9$ indicates an increase in back-bonding from the iron atom to the carbonyl ligand. Evidently, the GaR group is a worse π acceptor than the CO ligand. Consequently, in the IR spectra of C_{2v} symmetric **5** and **7** six red-shifted bands are observed in the carbonyl-stretching region between $\tilde{\nu} = 2026.1$ and 1917.7 cm^{-1} and $\tilde{\nu} = 2026.5$ and 1921.6 cm^{-1} , respectively. In addition an absorption for a bridging carbonyl ligand at $\tilde{\nu} = 1783.7$ cm^{-1} is also observed in **5** and **7**, which is 45 cm^{-1} lower than in $\text{Fe}_2(\text{CO})_9$. The chloride adduct **6** shows seven CO-absorption frequencies between $\tilde{\nu} = 2050.0$ and 1939.1 cm^{-1} for terminal CO ligands and a signal at 1817.8 cm^{-1} for the bridging CO group.

In the mass spectra of **4**, **5**, and **7** the molecule peaks are observed at highest mass. Prominent fragmentation pathways involve subsequent loss of up to six CO ligands. The mass spectrum of **5** shows no difference to that of **6**. Similarly in solution, the NMR spectra of **5** and **6** show the same chemical shifts for the CO and hypersilyl groups. This means **6** dissociates easily to form **5** and solvated sodium chloride.

Crystal structure analysis of $\text{Fe}_2(\text{CO})_9$ derivatives 4–6:

Compound **4** crystallizes in the hexagonal space group $P6_3/m$.^[16] A molecule of **4** resides on a site with $3/m$ symmetry (Figure 1). Three gallium atoms and two iron atoms form a trigonal bipyramidal cage with Ga–Fe distances of $238.18(7)$ pm. The iron atoms are coordinated in an octahedral fashion and the gallium centers have the coordination number three. The Ga–Ga distance of 328.9 pm is considerably longer than that in digallanes (234 – 255 pm)^[17] and in a cyclotrigallane dianion (244 pm).^[18] Thus, a Ga–Ga interaction appears inappropriate and **4** may be considered as a diiron enneacarbonyl analogue, in which bridging carbonyl ligands are replaced by for gallium hypersilyl groups. The Ga–Si bond of 238.7 pm is in the expected range for Ga–Si bond lengths (e.g., in **1** $d_{\text{Ga-Si}} = 239.5$ pm^[13] and in **2** $d_{\text{Ga-Si}} =$

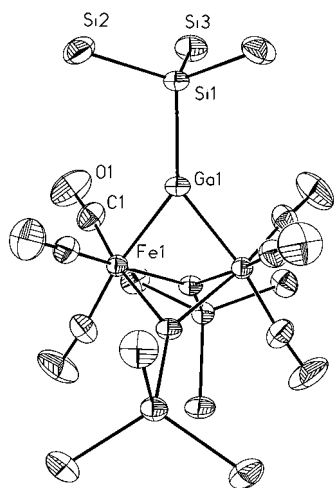


Figure 1. View of a molecule of **4**. The methyl groups have been omitted for clarity. Selected bond lengths [pm] and angles [°]: Ga1–Fe1 238.18(7), Ga1–Si1 238.7(2), Fe1–C1 177.6(5), Fe1–Fe1A 287.6(2), Si1–Si2 235.0(2), Si1–Si3 237.6(3); Fe1–Ga1–Fe1A 74.28(4), Fe1–Ga1–Si1 142.69(2), C1–Fe1–C1 99.0(2).

240.6 pm^[14]). The bond angles at the gallium centers deviate markedly from a trigonal planar arrangement; the Fe–Ga–Fe angle is acute, 74.28(4)°, and the Fe–Ga–Si angle is correspondingly wide, 142.69(2)°. The Fe–Fe distance (287.6(1) pm) is longer than in Fe₂(CO)₉, a consequence of the fact that Fe–Ga bonds are longer than Fe–C bonds; however, the compound is still diamagnetic.

In **5** (triclinic, space group *P* $\bar{1}$) only two bridging carbonyl ligands in the resulting Fe₂(CO)₉ type complex are substituted by GaR groups (Figure 2). The molecule consists of a Ga₂Fe₂

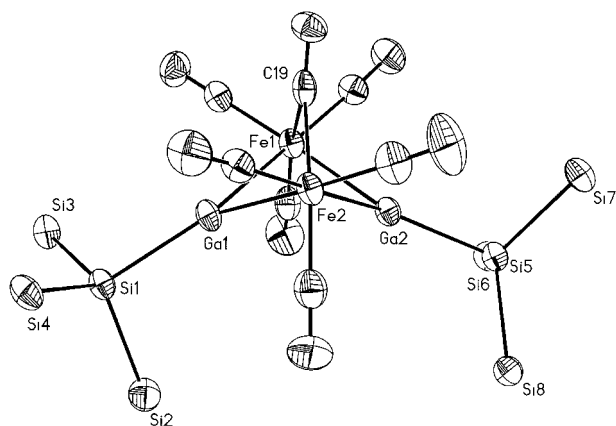


Figure 2. View of a molecule of **5**. The methyl groups have been omitted for clarity. Selected bond lengths [pm] and angles [°]: Ga1–Fe1 239.38(6), Ga1–Fe2 238.75(10), Ga2–Fe1 239.17(8), Ga2–Fe2 238.15(8), Fe1–Fe2 268.04(8), Ga1–Si1 238.54(9), Ga2–Si5 238.17(10), Fe1–C19 199.5(2), Fe2–C19 200.0(2), Fe–C_{term} 178.6(3)–180.1(2), Si–Si 234.9(1)–236.6(1), O19–C19 116.6(3); Fe2–Ga1–Fe1 68.19(2), Si1–Ga1–Fe1 149.86(2), Si1–Ga1–Fe2 141.71(3), Fe2–Ga2–Fe1 68.32(3), Si5–Ga2–Fe1 146.24(2), Si5–Ga2–Fe2 144.81(2), O19–C19–Fe1 138.8(2), O19–C19–Fe2 136.9(2), Fe1–C19–Fe2 84.28(9).

butterfly-shaped ring, with the Fe–Fe edge bridged by a CO ligand. The Ga1–Fe1–Fe2 and the Ga2–Fe1–Fe2 planes intersect at an angle of 58.2°, which deviates only slightly from the

60° angle of the GaFe₂ planes in **4**. The Ga–Fe bond lengths ($d_{\text{Ga-Fe}} = 238.9$ pm) are very similar to those of **4**. These Ga–Fe bond lengths in **4** and **5** are slightly shorter than most σ type Ga–Fe bonds, which lie around 245 (± 10) pm. For example, [CpFe(CO)₂]_{3–n}GaR_n ($n = 0, 1, 2$; $d_{\text{Ga-Fe}} = 241$ pm average)^[2] and [(thf)₂C₂H₃GaFe(CO)₄]₂ ($d_{\text{Ga-Fe}} = 251.5$ pm)^[5] have longer Ga–Fe bonds; however, the Ga–Fe bond length in [(CO)₂CpFeGaCl₂(NMe₃)] ($d_{\text{Ga-Fe}} = 236.18(3)$ pm) is even shorter.^[19]

Compound **6** (orthorhombic, space group *Pca*₂₁) has certain structural differences to **5** caused by the uptake of solvated sodium chloride (Figure 3). The GaFe₂ planes now intersect at

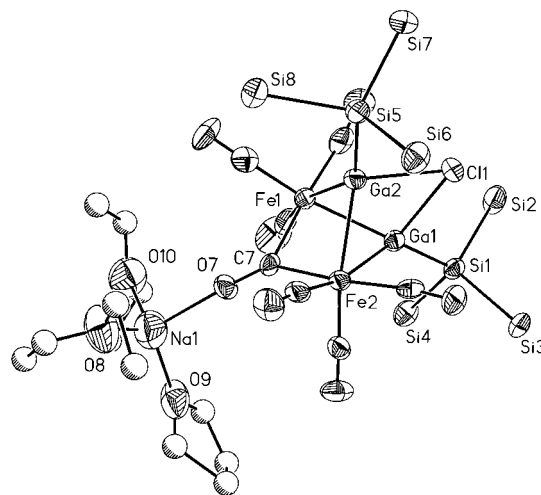


Figure 3. View of a molecule of **6**. The methyl groups have been omitted for clarity. Selected bond lengths [pm] and angles [°]: Ga1–Fe1 244.1(2), Ga1–Fe2 245.5(2), Ga2–Fe1 244.5(2), Ga2–Fe2 245.1(2), Ga1–Si1 239.2(3), Ga2–Si5 240.2(3), Ga1–Cl1 254.2(3), Ga2–Cl1 252.4(3), Fe–C_{term} 177.7(13)–181.6(13), Fe1–C7 194.1(9), Fe2–C7 193.5(8), Fe1–Fe2 267.9(2), Ga1–Ga2 291.5(1), Na1–O7 212.2(9), Si–Si 233.0(4)–235.8(4); Si1–Ga1–Fe1 141.97(8), Si1–Ga1–Fe2 139.39(8), Fe1–Ga1–Fe2 66.35(5), Si1–Ga1–Cl1 103.19(9), Fe1–Ga1–Cl1 97.52(7), Fe2–Ga1–Cl1 97.93(7), Si5–Ga2–Fe1 142.12(8), Si5–Ga2–Fe2 138.18(8), Fe1–Ga2–Fe2 66.35(5), Si5–Ga2–Cl1 103.65(9), Fe1–Ga2–Cl1 97.89(7), Fe2–Ga2–Cl1 98.50(7).

an angle of 90.7°. Thus, the Ga₂Fe₂ core is a distorted tetrahedron with the Ga–Ga edge bridged by a chlorine atom and the Fe–Fe edge bridged by a CO ligand. Consequently, the Ga–Ga distance (291.5(1) pm) is shorter than that in **5** (345.6 pm). The Fe–C7 distances are 6 pm shorter than those in **5**. As this is consistent with a longer C–O bond, stronger π back-bonding can be concluded. In a simple picture, this is a consequence of decreased π back-bonding from iron to gallium as a result of the p_z orbitals of the gallium atoms being blocked by chlorine coordination. The Ga–Fe bond lengths are also affected by the change in coordination number; on average they are elongated to 245 pm. The Ga–Cl bond lengths (av 253 pm) are longer than those usually observed in (R₂GaCl)₂ compounds ($d_{\text{Ga-Cl}} \approx 240$ pm).^[20] The sodium atom is coordinated tetrahedrally by two molecules of diethyl ether, one THF molecule, and the oxygen atom of the bridging carbonyl ligand.

Crystal structure analysis of 11: In **11** the Ga–Fe bonds (248.7 pm), which are classified as σ type, are of similar length

to those in **6**. Compound **11** (monoclinic, space group $P2_1/c$) is bicyclic and consists of a boat-shaped, six-membered Ga_3O_3 ring in which two gallium atoms are bridged by an $\text{Fe}(\text{CO})_4$ fragment (Figure 4). The iron atom has a distorted octahedral

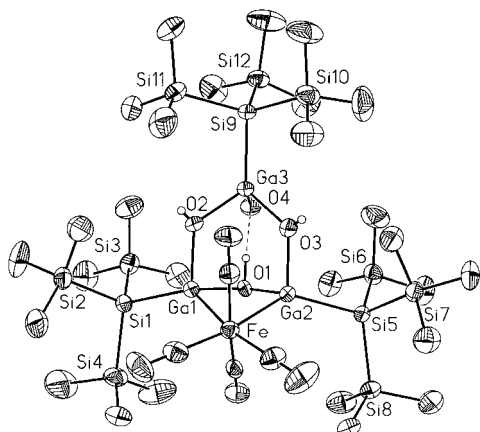


Figure 4. View of a molecule of **11**. Selected bond lengths [pm] and angles [°]: Fe–Ga1 248.36(12), Fe–Ga2 248.98(12), Ga1–Si1 240.1(2), Ga2–Si5 239.9(2), Ga3–Si9 238.5(2), Fe–C 177.6(8)–180.6(10), Ga1–O1 195.0(4), Ga1–O2 198.9(6), Ga2–O1 195.1(4), Ga2–O3 199.0(6), Ga3–O3 191.2(7), Ga3–O2 192.3(6), Ga3–O4 192.3(7), Si–Si 234.7(3)–235.8(3); Ga1–Fe–Ga2 71.59(4), O1–Ga1–O2 91.2(2), O1–Ga1–Si1 117.96(13), O2–Ga1–Si1 105.9(2), O1–Ga1–Fe 92.26(14), O2–Ga1–Fe 110.8(2), Si1–Ga1–Fe 131.44(6), O1–Ga2–O3 90.1(2), O1–Ga2–Si5 118.25(12), O3–Ga2–Si5 105.6(2), O1–Ga2–Fe 92.04(13), O3–Ga2–Fe 110.7(2), Si5–Ga2–Fe 132.26(6), O3–Ga3–O2 95.5(3), O3–Ga3–O4 99.6(3), O2–Ga3–O4 98.6(3), O3–Ga3–Si9 118.3(2), O2–Ga3–Si9 118.9(2), O4–Ga3–Si9 121.0(2), Ga1–O1–Ga2 96.4(2), Ga3–O2–Ga1 124.7(3), Ga3–O3–Ga2 126.0(4).

coordination environment; the bond angles range from 71.6° (Ga1–Fe–Ga2) to 100.2° (C28–Fe–C29). The Fe–C bond lengths (178.7 pm average) are similar to those of the terminal Fe–C bonds found in **4**, **5**, and **6**, and are in the normal range for Fe–C(CO). The hypersilyl groups are in equatorial positions, thus hydrogen bonding is possible between O1 and O4 ($d_{\text{O1–O4}} = 276.9$ pm). The Ga–Si bond lengths are in the expected range, but the Ga3–Si9 bond is 1.5 pm shorter than the two other Ga–Si bonds; this is a result of three instead of two oxygen atoms being bound to gallium.

Crystal structure analysis of the Ga_2Fe_3 cluster compounds **8 and **9**:** Compound **8** (triclinic, space group $P\bar{1}$ and with two formula units in the asymmetric unit) is the sodium salt of a monoanionic Ga_2Fe_3 cluster. It has a trigonal bipyramidal framework of two gallium and three iron atoms (Figure 5). The $\text{Fe}(\text{CO})_3$ fragments are in equatorial positions, the Ga–hypersilyl units in apical positions, and one Fe–Fe edge is hydrogen-bridged. The gallium atoms reside, approximately centered, 192 pm above and below the almost regular triangle of iron atoms; the deviation of the Ga–Ga axis from orthogonality is 1.5° and 2.7° in molecules 1 and 2, respectively. (Only molecule 1 will be discussed further as the arguments are valid for both molecules.) This small distortion causes differences in the Ga–Fe bonds lengths, 242.3 to 251.0 pm in molecule 1 [240.9 to 245.4 pm (molecule 2)], thus in terms of a classical description, this cluster might be considered as a derivative of $\text{Fe}_3(\text{CO})_{12}$. On the other hand this cluster might

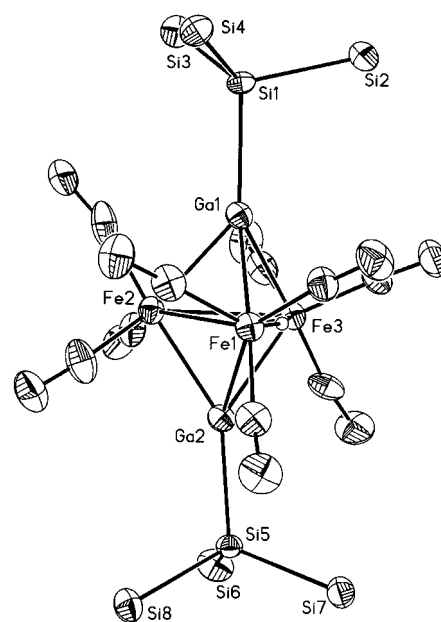


Figure 5. View of a Ga_2Fe_3 cluster ion of **8**. The methyl groups have been omitted for clarity. Selected bond lengths [pm] and angles [°]: Ga1–Fe1 246.4(2), Ga1–Fe3 247.0(2), Ga1–Fe2 248.0(2), Ga2–Fe2 242.3(2), Ga2–Fe3 249.4(2), Ga2–Fe1 251.0(2), Ga2–Si5 243.7(3), Ga1–Si1 245.9(3), Fe1–Fe2 267.2(2), Fe1–Fe3 271.4(2), Fe2–Fe3 274.9(3), Fe–C 171(1)–185(2), Si–Si 232.9(4)–236.1(4); Si1–Ga1–Fe1 141.46(9), Si1–Ga1–Fe3 142.76(9), Si1–Ga1–Fe2 137.60(9), Fe1–Ga1–Fe3 66.75(6), Fe1–Ga1–Fe2 65.44(6), Fe3–Ga1–Fe2 67.48(7), Fe2–Ga2–Si5 149.48(9), Fe2–Ga2–Fe3 67.98(7), Si5–Ga2–Fe3 134.98(9), Fe2–Ga2–Fe1 65.57(6), Si5–Ga2–Fe1 136.54(9), Fe3–Ga2–Fe1 65.68(6), Ga1–Fe1–Ga2 100.66(6), Ga1–Fe2–Ga2 102.68(7), Ga1–Fe3–Ga2 100.95(7), Fe2–Fe1–Fe3 61.38(7), Fe1–Fe2–Fe3 60.05(6), Fe1–Fe3–Fe2 58.56(6), Ga–Fe1–Fe2 54.78(5)–58.79(6).

be described, in accordance with Wade's rules, as a *closo*-polyhedron. The counterion is sodium coordinated by triglyme and two additional CO groups from two cluster molecules. Thus sodium is six coordinate in a strongly distorted trigonal prismatic environment. The isocarbonyl coordination gives rise to infinite cluster–Na–cluster chains parallel to c (Figure 6). The Na–O bond lengths to the CO groups are 235(1)–241(1) pm, which are longer than in **6** as a result of the increase in coordination number of four to six.

Anionic **9** (Figure 7) with counterion **10** (Figure 8) crystallizes in the monoclinic space group $P2_1/c$. Anion **9** has a distorted trigonal bipyramidal framework of $\text{Fe}(\text{CO})_3$ and Ga–hypersilyl groups similar to that in **8**; the structures of the Ga_2Fe_3 cores are nearly identical. If the $\text{Fe}(\text{CO})_3$ groups in **8** and **9** are superimposed, the gallium positions differ only by 6.9 and 11.5 pm. In **9** the Ga–Fe bonds range between 237.9 and 254.7 pm. The shortest Ga–Fe bond length lies opposite the bridged Fe–Fe edge. The bridging ligand in **9** is $\text{GaFe}(\text{CO})_4$; the average Ga–Fe($\text{CO})_3$ bond length is 245 pm. In contrast, the Ga–Fe bond length to the terminal $\text{Fe}(\text{CO})_4$ group is markedly shorter ($d_{\text{Ga–Fe}} = 228.9(1)$ pm). This very short Ga–Fe bond indicates extensive π bonding and will be discussed below. Here, the Ga atom is in an apical position, with a Ga–Fe4– C_{ap} angle of 177.8° .

The counterion **10** has an adamantoid Ga_4O_6 framework. The average Ga–O distance is 191.1 pm. The disorder^[21] of the Ga_4O_6 cage prevents a distinction between oxo and

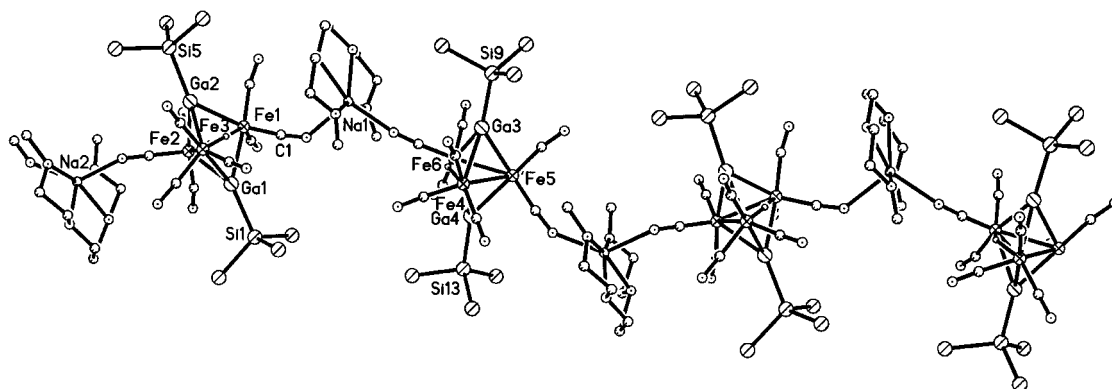
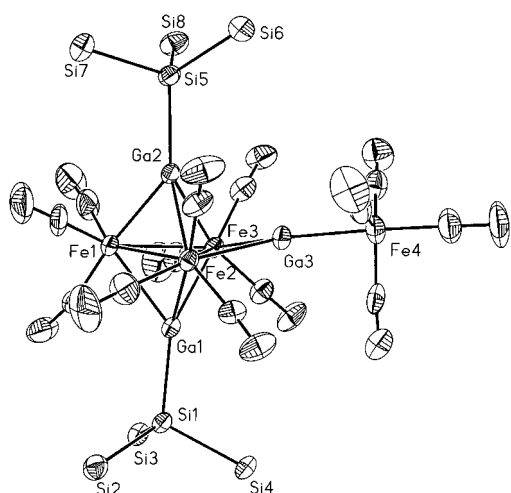
Figure 6. View of a $[8\text{-Na}(\text{triglyme})]_{\infty}$ chain.

Figure 7. View of a molecule of **9**. The methyl groups have been omitted for clarity. Selected bond lengths [pm] and angles [°]: Ga1–Fe1 254.7(1), Ga1–Fe2 244.4(1), Ga1–Fe3 245.4(1), Ga2–Fe1 237.9(1), Ga2–Fe2 253.0(1), Ga2–Fe3 252.5(1), Ga3–Fe2 246.1(1), Ga3–Fe3 244.6(1), Ga3–Fe4 228.9(1), Fe1–Fe2 270.8(1), Fe1–Fe3 269.7(1), Fe2–Fe3 274.9(1), Ga1–Si1 241.2(2), Ga2–Si5 241.0(2), Fe–C 171.3(9)–178.4(8), Si–Si 235.4(3)–237.2(3), Si1–Ga1–Fe1 137.35(5), Si1–Ga1–Fe2 141.19(6), Si1–Ga1–Fe3 143.28(6), Fe2–Ga1–Fe1 65.68(4), Fe2–Ga1–Fe3 68.28(4), Fe3–Ga1–Fe1 65.23(4), Fe1–Ga2–Si5 139.32(5), Fe1–Ga2–Fe3 66.65(4), Si5–Ga2–Fe3 141.34(6), Fe1–Ga2–Fe2 66.88(4), Si5–Ga2–Fe2 141.55(6), Fe3–Ga2–Fe2 65.88(3), Fe4–Ga3–Fe3 146.03(5), Fe4–Ga3–Fe2 144.85(5), Fe3–Ga3–Fe2 68.14(4), Ga2–Fe1–Ga1 102.46(4), Ga1–Fe2–Ga2 101.14(4), Ga1–Fe3–Ga2 101.00(4), Ga1–Fe2–Ga3 94.39(4), Ga3–Fe2–Ga2 78.80(4), Ga3–Fe3–Ga1 94.51(4), Ga3–Fe3–Ga2 79.19(4), Ga3–Fe2–Fe1 113.15(5), Ga3–Fe2–Fe3 55.67(3), Ga1,2–Fe–Fe 55.32(3)–59.23(4), Fe3–Fe1–Fe2 61.14(3), Fe1–Fe2–Fe3 59.23(3), Fe1–Fe3–Fe2 59.63(3).

hydroxo bridges. The hydroxyl protons could not be resolved. Other gallium oxo/hydroxo cages have been described, such as the adamantane type $[(\text{Me}_3\text{Si})_3\text{CGa}]_4\text{O}_2(\text{OH})_4$ ($d_{\text{Ga-O}} = 189.5(1)$ pm),^[22] $[\text{Me}_6\text{Ga}_6\text{O}_4(\text{OH})_4]$ ^[23] with an octahedral Ga core, and $[\text{Ga}_{12}\mu\text{Bu}_{12}(\mu_3\text{-O})_8(\mu\text{-O})_2(\mu\text{-OH})_4]$.^[24]

Density functional calculations: In **4–7** CO bridging ligands in $\text{Fe}_2(\text{CO})_9$ are substituted by hypersilyl gallium fragments. Density functional (DFT) calculations on several gallium substituted iron carbonyl compounds have been performed to evaluate the bonding situation. In all cases GaH derivatives have been chosen. In GaH the gallium–hydrogen bond is 170.7 pm. The lone pair at the gallium center occupies an

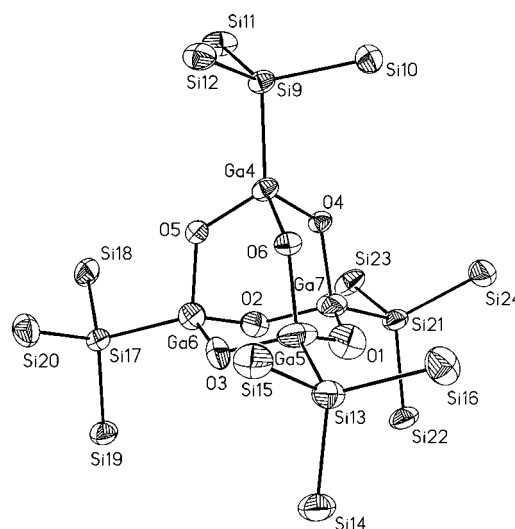


Figure 8. View of a molecule of **10**. The methyl groups have been omitted for clarity; average positions for split Ga and O atoms.

orbital that is slightly antibonding with regard to the GaH bond. This Ga–H distance is therefore shortened upon complexation to iron by approximately 10 pm. In addition the gallanediyl possesses two degenerate empty p orbitals, 2.5 eV above the HOMO at -2.56 eV, that might function as π acceptor orbitals. Thus GaH has a similar orbital situation to that in carbon monoxide, where the empty π^* orbitals are 7 eV above the HOMO at -1.98 eV.

The $\text{Fe}_2(\text{CO})_9$ derivatives $[(\text{CO})_3\text{Fe}(\mu\text{-GaH})_3\text{Fe}(\text{CO})_3]$ (**12**) and $[(\text{CO})_3\text{Fe}(\mu\text{-GaH})_2(\mu\text{-CO})\text{Fe}(\text{CO})_3]$ (**13**) have similar Ga–Fe bond lengths (Figure 9). Addition of a chloride ion to **13** into a Ga–Ga bridging position affords **14** with Ga–Fe bonds 7 pm longer. These calculated values fit well with the experimental results, that is, those that are obtained with the very bulky hypersilyl substituent. The two-center shared electron numbers (SEN) calculated by a Roby–Davidson population analysis,^[25] which give a rough measure of bond order, are 1.44 and 1.33 for the Ga–Fe bonds in **12** and **13**, respectively. Evidently, replacement of a GaH unit by a CO ligand results in a slight weakening of the Ga–Fe bond. The SEN for the Ga–Fe bonds in **14** is reduced to 1.28. For comparison **15**, with a terminal GaH ligand, has a Ga–Fe bond length of 220 pm and an SEN of 1.89. This value divides

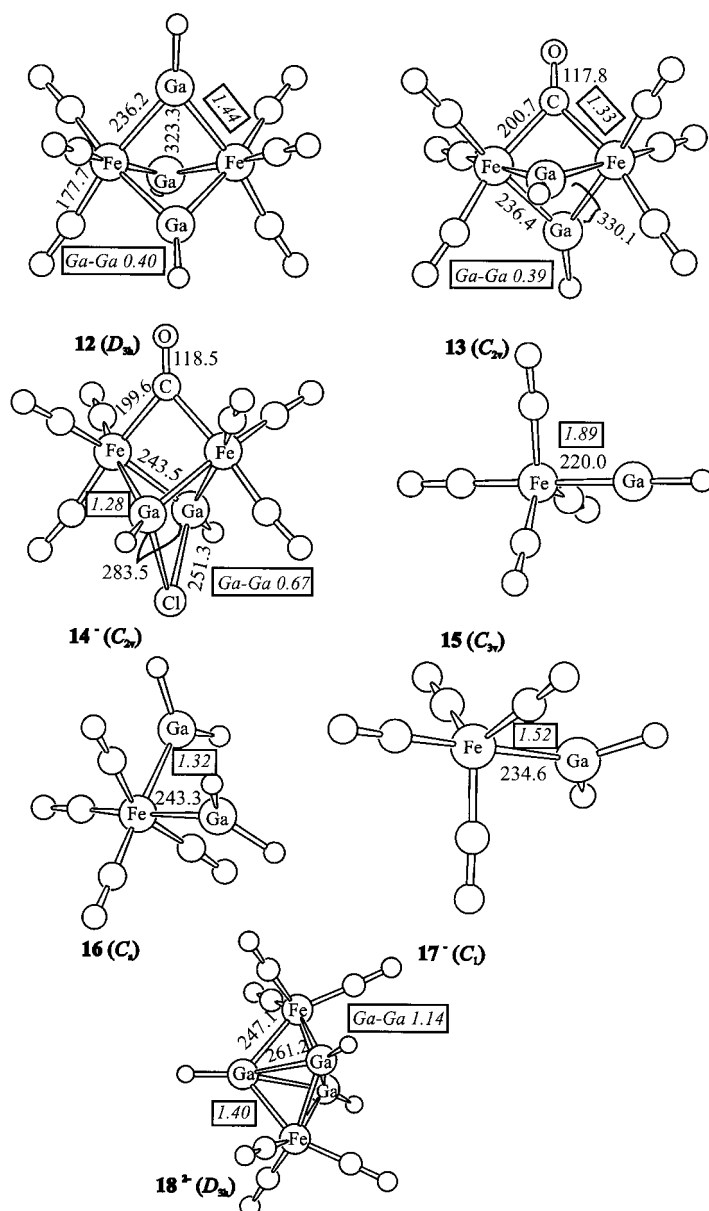


Figure 9. DFT calculated structures and selected SEN's of **12**–**18**.

into an SEN of 1.19 for the σ bond and shares of 0.35 each for the two degenerate π -type orbitals. This resembles the situation for terminal CO ligands. For the CO ligand in the apical position in **15** and $\text{Fe}(\text{CO})_5$ an SEN of 1.52 (1.50) is calculated that can also be split into σ (1.20) and π terms (2×0.16). In all cases an increase of the positive charge on the ligating atoms of CO and GaH is observed compared with that of the free ligands. This is in agreement with a strong electron donation from the ligands to the metal center and weaker back-bonding. The calculated Ga–Fe bond length in **15** is in good agreement with the experimental value for arylGaFe(CO)₄ ($d_{\text{Ga-Fe}} = 222.48(7)$ pm, aryl = 2,6-bis(2,4,6-triisopropylphenyl)phenyl).^[7a] Nevertheless, the Ga–Fe bond is predominantly a donor bond from the gallanediyl to the iron fragment, and the short bond length may be explained mainly by the low coordination number at the gallium center. From this point of view, there is no reason to postulate a Ga–

Fe triple bond in this compound, as Robinson et al. do. A similar conclusion was drawn in the meantime by Cotton et al. on the basis of spectroscopic data and DFT calculations.^[7b] The Ga–Fe bond length in **15** is shorter than that found in **9** for the $\text{Fe}(\text{CO})_4$ bound Ga atom, which as a result of its coordination number of three is not really part of a terminal RGa group. Its bonding situation is better modeled by the anionic complex $[(\text{CO})_4\text{FeGaH}_2]^-$ (**16**) with a Ga–Fe distance of 234.6 pm. Terminal GaH₂ groups in $[(\text{CO})_4\text{Fe}(\text{GaH}_2)_2]$ (**17**) have a Ga–Fe single-bond length of 243.3 pm. The trigonal bipyramidal cluster **8** formed from two $\text{Fe}(\text{CO})_3$ and two GaR units is isolobal to a singly protonated *closo*-B₅H₅²⁻ cluster^[26] and **18**. The latter results from a two-electron reduction of **12**, which has two framework electrons less. In **18** six framework electron pairs are available and, accordingly, **18** has Ga–Ga bond lengths comparable with those in **2**. This change in structure is also expressed by the SEN values. The value for the Ga–Fe bonds remains nearly unaffected, but in **18** a strong Ga–Ga interaction is found. The three-center SEN for the Ga–Ga–Fe faces of 0.42 signifies considerable electron delocalization in **18**, which is in agreement with a description of the bonding situation with multicenter bonds in **18** and with two-center bonds in **12**.

Conclusions

We have shown that various Ga–Fe clusters can be synthesized by the reaction of **1** with iron carbonylates. In these compounds the Ga–hypersilyl fragment can function as a CO ligand substitute in a $\mu_2(\text{Fe}–\text{Fe})$ bridging position in diiron enneacarbonyl derivatives. The gallanediyl fragment is also able to bind in a $\mu_3(\text{Fe}–\text{Fe}–\text{Fe})$ mode that results in polyhedral compounds following the Wade–Rudolph–Mingos cluster electron counting rules.

Experimental Section

General: All experiments were performed under purified nitrogen or in vacuo with Schlenk techniques. NMR: Bruker ACP200 and 250; Mass spectra: Varian MAT711 machines with direct inlet; IR: Bruker IFS 113V; X-ray crystallography:^[27] Suitable crystals were mounted with a perfluorated polyether oil on the tip of a glass fiber and cooled immediately on the goniometer head. Data collections were performed in ω scan with MoK α radiation (graphite monochromator) on STOE IPDS (**9**–**10**) and STADI4 (**5**, **8**, **11**) diffractometers and on a Siemens P4 diffractometer equipped with a SMART detector (**4**, **6**) and commercial software. Structures were solved and refined with the program package Siemens SHELXTL (PC) or SHELXL97. Refinement in full matrix against F^2 . All non-hydrogen atoms were refined anisotropically. All hydrogen atoms bound to carbon atoms were included as riding model with fixed isotropic U values in the final refinement. For further details see Table 1; Quantum chemical calculations: TURBOMOLE,^[28] split valence basis set for all atoms, BP86 functional, RI approximation. Gallium halides were prepared from the elements,^[29] $[\text{Li}(\text{thf})_3\text{Si}(\text{SiMe}_3)_3]$,^[12] $\text{Na}_2\text{Fe}(\text{CO})_4$,^[30] $\text{Na}_2\text{Fe}_2(\text{CO})_8$,^[29] and $\text{Na}_2\text{Fe}_3(\text{CO})_{11}$ ^[29] as described in the literature. Other chemicals were used as purchased.

Reaction of **1** with disodium tetracarbonylferrate (Collman's reagent).

A) A solution of **1** (0.45 g, 0.32 mmol) in diethyl ether (25 mL) was added dropwise at room temperature to a suspension of $\text{Na}_2\text{Fe}(\text{CO})_4 \cdot 2$ dioxane (0.22 g, 0.64 mmol), containing approximately 5% sodium hydroxide in diethyl ether (25 mL). The mixture was stirred for a further 24 h, filtered,

Table 1. Crystal data and data collection parameters.

	4	5	6	8	9·10	11
formula	C ₃₃ H ₈₁ Fe ₂ Ga ₃ O ₆ Si ₁₂	C ₂₃ H ₅₄ Fe ₂ Ga ₂ O ₇ Si ₈	C ₃₇ H ₈₂ ClFe ₂ Ga ₂ NaO ₁₀ Si ₈	C ₃₃ H ₇₃ Fe ₃ Ga ₂ NaO ₁₃ Si ₈	C ₆₇ H ₁₆₇ Fe ₄ Ga ₇ O ₁₉ Si ₂₄	C ₃₁ H ₈₅ FeGa ₃ O ₈ Si ₁₂
<i>M_r</i>	1231.92	942.54	1221.33	1256.63	2660.59	1188.08
crystal size [mm]	0.20 × 0.35 × 0.35	0.10 × 0.65 × 1.20	0.2 × 0.2 × 0.3	0.25 × 0.25 × 0.20	0.20 × 0.35 × 0.40	0.12 × 0.44 × 1.00
crystal system	hexagonal	triclinic	orthorhombic	triclinic	monoclinic	monoclinic
space group	<i>P</i> 6 ₃ / <i>m</i>	<i>P</i> $\bar{1}$	<i>Pca</i> 2 ₁	<i>P</i> $\bar{1}$	<i>P</i> 2 ₁ / <i>c</i>	<i>P</i> 2 ₁ / <i>c</i>
<i>a</i> [Å]	15.2112(1)	9.613(2)	27.9306(4)	16.949(3)	18.899(4)	9.326(1)
<i>b</i> [Å]	15.2112(1)	14.615(3)	9.54550(10)	19.098(4)	17.391(4)	28.102(3)
<i>c</i> [Å]	16.2064(2)	16.822(3)	23.8385(2)	22.714(5)	42.405(9)	24.605(2)
α [°]	90.00	84.23(3)	90.00	96.17(3)	90.00	90.00
β [°]	90.00	85.44(3)	90.00	111.47(3)	101.94(3)	100.044(8)
γ [°]	120.00	75.79(3)	90.00	112.22(3)	90.00	90.00
<i>V</i> [Å ³]	3247.46(5)	2275.8(8)	6355.62(12)	6071(2)	13 636(5)	6349.6(11)
<i>Z</i>	2	2	4	4	4	4
ρ_{calcd} [kg m ⁻³]	1.260	1.375	1.276	1.375	1.296	1.243
μ [mm ⁻¹]	1.917	2.040	1.527	1.788	2.027	1.744
<i>F</i> (000)	1280	972	2552	2600	5504	2488
index range	$\pm h \pm k \pm l$	$\pm h \pm kl$	$\pm h \pm k \pm l$	$\pm h \pm kl$	$\pm h \pm k \pm l$	$\pm hkl$
$2\theta_{\text{max}}$ [°]	48	60.00	46.5	45.10	47.9	45
<i>T</i> [K]	210	200	193(2)	293(2)	200	200
refl. collected	15201	14 719	26284	12991	63 021	5443
refl. unique	1773	13 037	8806	12991	20 017	5443
refl. observed (4 σ)	1644	11 049	7841	10 511	10 871	4194
<i>R</i> (int.)	0.0996	0.0159	0.0575	0.0000	0.0569	0.0000
absorption correction	semiempirical	numerical	semiempirical	semiempirical	numerical	semiempirical
min/max transmission	0.4785/0.5710	0.1669/0.5715	0.16415/0.21959	0.239/0.450	0.246/0.485	0.4076/0.6892
parameters	110	415	572	1256	1174	538
weighting scheme ^[a] / <i>w</i>	0.0427/0.8976	0.0513/0.9474	0.0077/17.2154	0.1207/36.4562	0.0654/0.0000	0.0344/6.9700
GOOF	1.197	1.065	1.272	1.150	0.858	1.152
<i>R</i> (4 σ)	0.038	0.034	0.0675	0.0492	0.049	0.035
<i>wR</i> ₂	0.085	0.102	0.1181	0.1401	0.122	0.095
larg. res. peak [e Å ⁻³]	0.504	0.631	0.398	1.092	0.847	0.411

$$[a] w^{-1} = \sigma^2 F_o^2 + (xP)^2 + yP; P = (F_o^2 + 2F_c^2)/3$$

and the solution reduced to a volume of 3 mL. Compound **4** crystallized as yellow prisms (0.16 g; 41 % with respect to Na₂Fe(CO)₄) at 0 °C. From the mother liquor black crystals of **9·10** (0.06 g, 14 %) grew at room temperature, which were washed with pentane. The resulting solution was reduced to 5 mL and **11** (0.02 g) were obtained as colorless crystals.

B) A suspension of donor-free Na₂Fe(CO)₄ (0.40 g, 1.87 mmol) in a solution of **1** (0.99 g, 0.70 mmol) in diethyl ether (50 mL) was stirred for 4 d. The orange–red mixture was filtered and the solution reduced to 10 mL. Upon cooling the mixture to 0 °C of **4** (0.71 g; 61 %) crystallized in several portions.

Compound **4**: ¹H NMR (C₆D₆): δ = 0.40; ¹³C NMR (C₆D₆): δ = 214.3 (CO), 4.2 (CH₃); ²⁹Si NMR (C₆D₆): δ = –89.5 (*Si*(SiMe₃)₃), –7.1 (SiMe₃); MS (70 eV, EI, ⁶⁹Ga): *m/z* (%): 1232 (26) [M]⁺, 774 (36) [Fe(CO)₃(GaSi(SiMe₃)₃)₂]⁺, 316 (66) [GaSi(SiMe₃)₃]⁺, 73 (100) [SiMe₃]⁺; IR (KBr): ν (CO) = 1964 (s), 1921 cm⁻¹ (s).

Compound **9·10**: ¹H NMR ([D₈]THF): δ = 0.31 (54H, FeGaSi(SiMe₃)₃), 0.30, 0.29, 0.28, 0.27 (27H, SiMe₃). The solubility of **9·10** was too low to obtain well-resolved ²⁹Si and ¹³C NMR spectra.

Compound **11**: ¹H NMR (C₆D₆): δ = 2.00 (br, 4H; OH) 0.44 (54H; FeGaSi(SiMe₃)₃), 0.30 (27H; SiMe₃); ¹³C NMR (C₆D₆): δ = 4.3 (FeGaSi(SiMe₃)₃), 4.1 (O₃GaSi(SiMe₃)₃); ²⁹Si NMR (C₆D₆): δ = –119.5 (FeGaSi(SiMe₃)₃), (O₃GaSi(SiMe₃)₃; not observed), –8.2 (SiMe₃); MS (70 eV, EI, ⁶⁹Ga): *m/z* (%): 1166 (14) [M – H₂O]⁺, 901 (6) [M – 2H₂O – Si(SiMe₃)₃]⁺, 247 (19) [Si(SiMe₃)₃]⁺, 18 (100) [H₂O]⁺.

Reaction of 1 with Na₂Fe₂(CO)₈: A solution of **1** (0.45 g, 0.32 mmol) in THF (10 mL) was added dropwise to a suspension of Na₂Fe₂(CO)₈ (0.25 g, 0.65 mmol) in THF (25 mL). An orange–red solution formed, which was stirred for 2 h. Then all volatiles were removed in vacuo and the residue was dispersed in diethyl ether (25 mL). The mixture was filtered and concentrated to 5 mL. Compound **6** (0.34 g; 43 %) crystallized at 0 °C. ¹H NMR (C₆D₆): δ = 3.52 (m, 4H; OCH₂^{THF}), 3.26 (q, 8H; OCH₂CH₃), 1.41 (m, 4H; CH₂^{THF}), 1.10 (t, 12H; OCH₂CH₃), 0.32 (s, 54H; SiMe₃); ¹³C NMR

(C₆D₆): δ = 216.0 (CO), 66.6 (OCH₂CH₃), 16.2 (OCH₂CH₃), 4.0 (SiMe₃), (THF signals not observed); ²⁹Si NMR (C₆D₆): δ = –84.1 (*Si*(SiMe₃)₃), –7.2 (SiMe₃); MS (70 eV, EI, ⁶⁹Ga): *m/z* (%): 942 (82) [M]⁺, 914 (26) [M – CO]⁺, 886 (11) [M – 2CO]⁺, 858 (34) [M – 3CO]⁺, 830 (100) [M – 4CO]⁺ [M = 6 – Na(OEt)₂(thf)Cl]; IR (KBr): ν (CO) = 2023.1 (s), 2005.0 (s), 1995.1 (s), 1983.7 (s), 1976.7 (sh), 1939.1(s), 1817.8 cm⁻¹ (w).

Reaction of 1 with Na₂Fe₃(CO)₁₁: A solution of **1** (0.47 g, 0.34 mmol) in THF (15 mL) was added at –78 °C to a suspension of Na₂Fe₃(CO)₁₁·0.5 triglyme (0.43 g, 0.70 mmol) in THF (50 mL). After slowly warming to ambient temperature the mixture was stirred for additional 4 h. Then all volatiles were removed in vacuo and the residue was taken up in pentane. Subsequent filtration afforded an orange-red solution from which **5** (0.19 g; 30 % with respect to Ga) crystallized in several portions. Compound **7** (0.02 g; 2 %) crystallized from the mother liquor. The residue of filtration was extracted with THF (50 mL) and filtered. The dark red solution was concentrated to 10 mL. Black crystals of **8** (0.37 g, 42 %) were formed at –78 °C.

Compound **5**: ¹H NMR (C₆D₆): δ = 0.32; ¹³C NMR (C₆D₆): δ = 216.0 (CO), 4.0 (SiMe₃); ²⁹Si NMR (C₆D₆): δ = –84.1 (*Si*(SiMe₃)₃), –7.2 (SiMe₃); MS (70 eV, EI, ⁶⁹Ga): identical to that of **6**; IR (KBr): ν (CO) = 2026.1 (s), 1999.3 (s), 1971.4 (s), 1961.5 (s), 1947.7 (s), 1919.7 (s), 1783.7 cm⁻¹ (s).

Compound **7**: MS (70 eV, EI, ⁶⁹Ga): *m/z* (%): 652 (31) [M]⁺, 624 (9) [M – CO]⁺, 596 (26) [M – 2CO]⁺, 568 (86) [M – 3CO]⁺, 540 (44) [M – 4CO]⁺, 512 (26) [M – 5CO]⁺, 484 (92) [M – 6CO]⁺, 316 (100) [GaSi(SiMe₃)₃]⁺; IR (KBr): ν (CO) = 2026.5 (m), 2001.4 (s), 1972.6 (s), 1961.6 (sh), 1948.1 (s), 1921.6 (s), 1784.9 cm⁻¹ (s).

Compound **8**: ¹H NMR ([D₈]THF): δ = 3.55 (s, 4H; MeO(CH₂)₂OCH₂), 3.29 (s, 6H; OMe), 0.27 (s, 54H; SiMe₃), –16.9 (s, 1H; FeH); ¹³C NMR ([D₈]THF): δ = 4.0 (SiMe₃); ²⁹Si NMR ([D₈]THF): δ = –125.0 (*Si*(SiMe₃)₃), –9.0 (SiMe₃); IR (KBr): ν (CO) = 2009.1 (w), 1970.5 (s), 1956.3 (m), 1942.7 (s), 1920.1 (m), 1914.4 (s), 1902.5 (m), 1888.3 (m), 1873.2 cm⁻¹ (m).

Acknowledgments: We thank the Deutsche Forschungsgemeinschaft, the Fonds der Chemischen Industrie, the Chemetall GmbH, and Prof. H. Schnöckel for supporting this work as well as Prof. H. Nöth (and his co-workers Dr. H. Schwenk, J. Knizek) and Prof. P. Klüfers (H. Piotrowski) for collecting X-ray data sets.

Received: November 4, 1997 [F876]

- [1] M. J. Taylor, *Metal-to-Metal Bonded States of the Main Group Elements*, Academic Press, London, **1975**, chap. 3.
- [2] a) R. M. Campbell, L. M. Clarkson, W. Clegg, D. C. R. Hockless, N. L. Arkett, N. C. Norman, *Chem. Ber.* **1992**, *125*, 55–58; b) X. He, R. A. Bartlett, P. P. Power, *Organometallics* **1994**, *13*, 548–552.
- [3] R. A. Fischer, A. Miehr, M. M. Schulte, *Adv. Mater.* **1995**, *7*, 58–61.
- [4] R. A. Fischer, M. M. Schulte, E. Herdtweck, M. R. Mattner, *Inorg. Chem.* **1997**, *36*, 2010–2017.
- [5] J. C. Vanderhooff, R. D. Ernst, F. W. Cagle, Jr., R. J. Neustadt, T. H. Cymbaluk, *Inorg. Chem.* **1982**, *21*, 1876–1880.
- [6] R. A. Fischer, M. M. Schulte, T. Priermeier, *J. Organomet. Chem.* **1995**, *493*, 139–142.
- [7] a) J. Su, X.-W. Li, R. C. Crittendon, C. F. Campana, G. H. Robinson, *Organometallics* **1997**, *16*, 4511–4513; b) F. A. Cotton, X. Feng, *ibid.* **1998**, *17*, 128.
- [8] $[(\text{CO})_5\text{CrGaCl}(\text{thf})_2]$ and $[\text{Ru}\{\text{GaCl}(\text{thf})_2\}\{\text{GaCl}_2(\text{thf})_2\}(\text{CO})_3] \cdot 0.5\text{THF}$ with terminal coordination of a gallium(i) species, though as donor adducts with coordination number four, have been reported: a) M. M. Schulte, E. Herdtweck, G. Rauschdahl-Sieber, R. A. Fischer, *Angew. Chem.* **1996**, *108*, 489–491; *Angew. Chem. Int. Ed. Engl.* **1996**, *35*, 424–426; b) G. N. Harakas, B. R. Whittlesey, *Inorg. Chem.* **1997**, *36*, 2704–2707.
- [9] J. Weiss, D. Stetzkamp, B. Nuber, R. A. Fischer, C. Boehme, G. Frenking, *Angew. Chem.* **1997**, *109*, 95–97; *Angew. Chem. Int. Ed. Engl.* **1997**, *36*, 70–72.
- [10] C. Dohmeier, H. Krautscheid, H. Schnöckel, *Angew. Chem.* **1994**, *106*, 2570–2571; *Angew. Chem. Int. Ed. Engl.* **1994**, *33*, 2482–2483.
- [11] W. Uhl, M. Pohlmann, *Organometallics* **1997**, *16*, 2478–2480.
- [12] a) H. Gilman, C. L. Smith, *J. Organomet. Chem.* **1968**, *14*, 91–101; b) G. Gutekunst, A. G. Brook, *ibid.* **1982**, *225*, 1–3; c) A. Heine, R. Herbst-Irmer, G. M. Sheldrick, D. Stalke, *Inorg. Chem.* **1993**, *32*, 2694–2698.
- [13] G. Linti, W. Köstler, *Angew. Chem.* **1996**, *108*, 593–595; *Angew. Chem. Int. Ed. Engl.* **1996**, *35*, 550–552.
- [14] G. Linti, W. Köstler, A. Rodig, *Eur. J. Inorg. Chem.* **1998**, *1*, in press.
- [15] G. Linti, *J. Organomet. Chem.* **1996**, *520*, 107–113.
- [16] The crystals of **4** are merohedrally twinned, thus giving the impression of a higher symmetric space group $P6_322$. This was taken into consideration in the structure refinement by twin refinement.
- [17] a) W. Uhl, *Angew. Chem.* **1993**, *105*, 1449–1461; *Angew. Chem. Int. Ed. Engl.* **1993**, *32*, 1386–1397; b) C. Dohmeier, D. Loos, H. Schnöckel, *ibid.* **1996**, *108*, 141–161 and **1996**, *35*, 129–149; c) N. Wiberg, K. Amelunxen, H. Nöth, H. Schwenk, W. Kaim, A. Klein, T. Scheiring, *ibid.* **1997**, *109*, 1258–1261 and **1997**, *36*, 1213–1215.
- [18] a) X.-W. Li, W. T. Pennington, G. H. Robinson, *J. Am. Chem. Soc.* **1995**, *117*, 7578–7580; b) X.-W. Li, Y. Xie, P. R. Schreiner, K. D. Gripper, R. C. Crittendon, C. F. Campana, H. F. Schaefer, G. H. Robinson, *Organometallics* **1996**, *15*, 3798–3803.
- [19] R. A. Fischer, A. Miehr, T. Priermeier, *Chem. Ber.* **1995**, *128*, 831–843.
- [20] M. A. Petrie, P. P. Power, H. V. R. Dias, K. Ruhlandt-Senge, K. M. Waggoner, R. J. Wehmschulte, *Organometallics* **1993**, *12*, 1086–1093.
- [21] The Ga_3O_6 core is disordered (1:1 ratio). Only the Ga and O atom positions are split; for the substituents no split positions could be resolved. The split O atoms were refined only isotropically. In averaged positions these O atoms were refined anisotropically; the R values were virtually unaffected.
- [22] C. Schnitter, H. W. Roesky, T. Albers, H.-G. Schmidt, C. Röpken, E. Parisini, G. M. Sheldrick, *Chem. Eur. J.* **1997**, *3*, 1783–1792.
- [23] J. Storre, T. Belgardt, D. Stalke, H. W. Roesky, *Angew. Chem.* **1994**, *106*, 1365–1366; *Angew. Chem. Int. Ed. Engl.* **1994**, *33*, 1244–1245.
- [24] C. C. Landry, C. J. Harlan, S. G. Bott, A. R. Barron, *Angew. Chem.* **1995**, *107*, 1315–1317; *Angew. Chem. Int. Ed. Engl.* **1995**, *34*, 1201–1203.
- [25] E. R. Davidson, *J. Chem. Phys.* **1967**, *46*, 3320–3324; K. R. Roby, *Molec. Phys.* **1974**, *27*, 81–89; R. Heinzmann, R. Ahlrichs, *Theoret. Chim. Acta* **1976**, *42*, 33–45.
- [26] P. von R. Schleyer, G. Subramanian, A. Dransfeld, *J. Am. Chem. Soc.* **1996**, *118*, 9988–9989.
- [27] Further details of the crystal structure investigations can be obtained from the Fachinformationszentrum Karlsruhe, D-76344 Eggenstein-Leopoldshafen (Germany); fax (+49) 7247-808-666; e-mail: crysdata@fiz.karlsruhe.de) on quoting the depositary numbers CSD-407870 (4), CSD-407871 (5), CSD-407872 (6), CSD-407873 (8), CSD-407874 (9•10), and CSD-407875 (11).
- [28] R. Ahlrichs, M. Häser, Universität Karlsruhe **1996**.
- [29] Brauer, *Handbuch der präparativen Anorganischen Chemie*, F. Enke, Stuttgart, **1975**.
- [30] H. Strong, P. J. Krusic, J. San Filippo, Jr., *Inorg. Synthesis* **1990**, *28*, 203–206.